Are plasma bubbles a prerequisite for the formation of broad plasma depletions in the equatorial *F* region?

Hyosub Kil[1] and Woo Kyoung Lee[1,2]

Received 4 June 2013; accepted 21 June 2013; published 21 July 2013.

[1] Formation of broad plasma depletions (BPDs) at night in the equatorial *F* region is understood in association with plasma bubbles. However, we report BPDs that do not show a connection with bubbles. The characteristics of BPDs are investigated using the observations of the Communication/Navigation Outage Forecasting System (C/NOFS) satellite on 31 December 2008, 28 July 2010, and 1 February 2011. On those days, BPDs are detected in the longitude regions where C/NOFS did not detect bubbles prior to the detection of BPDs. The coincident C/NOFS and radar observations over Jicamarca in Peru show the occurrence of BPDs at the time when backscatter echoes are absent and at the height below backscatter echoes. These observations indicate that bubbles are not a prerequisite for those BPDs. The detections of those BPDs can be explained by the uplift of the equatorial *F* region peak height above the satellite orbit. **Citation:** Kil, H., and W. K. Lee (2013), Are plasma bubbles a prerequisite for the formation of broad plasma depletions in the equatorial *F* region?, *Geophys. Res. Lett.*, *40*, 3491–3495, doi:10.1002/grl.50693.

1. Introduction

[2] Broad plasma depletions (BPDs), plasma depletions of several hundred kilometers in longitude with respect to the background, have been observed in the nighttime equatorial *F* region during large geomagnetic storms [*Basu et al*., 2007; *Burke et al*., 2009; *Greenspan et al*., 1991; *Kil et al*., 2006; *Kil and Paxton*, 2006, *Su et al*., 2002]. BPDs are much wider than small-scale depletions known as "bubbles" and are considered to be created by a mechanism that is different from the creation mechanism of bubbles. Since its launch in April 2008, the Communication/Navigation Outage Forecasting System (C/NOFS) satellite detected many BPDs during both magnetically quiet periods and magnetically disturbed periods. BPDs are often observed with bubbles, and naturally, there have been efforts to understand the formation of BPDs in association with bubbles [*Burke et al*., 2009; *Huang et al*., 2011, 2012; *Kil et al*., 2006; *Kil and Paxton*, 2006]. From the observations of widening of plasma depletions with time, *Huang et al*. [2011, 2012] suggested a merger of bubbles as the cause of BPDs. This view is different from the interpretation of BPDs in terms of the uplift of the *F* region [*Basu et al*., 2007; *de La Beaujardière et al*., 2009; *Greenspan et al*., 1991; *Su et al*., 2002].

[3] As described above, the source of BPDs is still under debate. The formation mechanisms of BPDs can be different during magnetically disturbed and quiet periods and case by case. Many BPD events detected by C/NOFS are expected to elucidate the characteristics and source of the BPD phenomenon. As a part of this effort, we investigate the causal relationship between bubbles and BPDs using C/NOFS and radar observations. Through this investigation, we aim at addressing the following question: Are bubbles a prerequisite for the creation of BPDs? The occurrence and evolution of BPDs are investigated with the C/NOFS observations on 31 December 2008 ($Kp = 3^+$), 28 July 2010 ($Kp = 4^o$), and 1 February 2011 ($Kp = 3^-$). Days are based on universal time (UT). For the BPD event on 31 December 2008 over Jicamarca in Peru, we investigate the association of BPDs with plumes and an irregularity layer on the bottomside of the *F* region.

2. Observations and Discussion

[4] The C/NOFS satellite was launched in April 2008 into a low-inclination (13°) elliptical (altitude: 400–850 km) orbit. Coupled Ion-Neutral Dynamics Investigation (CINDI) is one of the payloads for the C/NOFS program, and this study uses the measurements of the ion density by CINDI. The data sampling cadence of CINDI is 0.5 s. Jicamarca Unattended Long-Term Investigations of the Ionosphere and Atmosphere (JULIA) is a low-power 50 MHz coherent scatter radar located at the Jicamarca Radio Observatory (JRO) [*Hysell and Burcham*, 1998]. The occurrence time, height, and movement of irregularities are investigated using the measurements of the Doppler velocity of the backscatter echoes by JULIA.

[5] We have searched for BPD events over JRO during the operation periods of JULIA since the C/NOFS launch and found one event on 31 December 2008. The CINDI and JULIA observations are presented in Figure 1. Three C/NOFS orbits are shown on the map in Figure 1a. The location of JRO (11.95°S, 76.87°W) is marked with a black solid dot, and the magnetic equator is shown with a black dashed line. The CINDI ion densities (log scale) and C/NOFS altitudes (linear scale) along the three C/NOFS orbits are shown in Figures 1b–1d. The CINDI data points are shown with red dots. The black, yellow, and green colors on the altitude curves (thick solid lines) indicate the LT intervals of 1800–2200, 2200–0200, and 0200–0600, respectively. The heights of the C/NOFS orbits projected onto the magnetic equator along the magnetic field lines (apex heights) are shown with black dashed lines. Figure 1g shows the map of the vertical Doppler velocity of backscatter echoes observed by JULIA. The altitude-average zonal (positive is eastward) and vertical

[1]The Johns Hopkins University Applied Physics Laboratory, Laurel, Maryland, USA.
[2]Korea Astronomy and Space Science Institute, Daejeon, South Korea.

Corresponding author: H. Kil, The Johns Hopkins University Applied Physics Laboratory, 11100 Johns Hopkins Rd., Laurel, MD 20723, USA. (hyosub.kil@jhuapl.edu)

0094-8276/13/10.1002/grl.50693

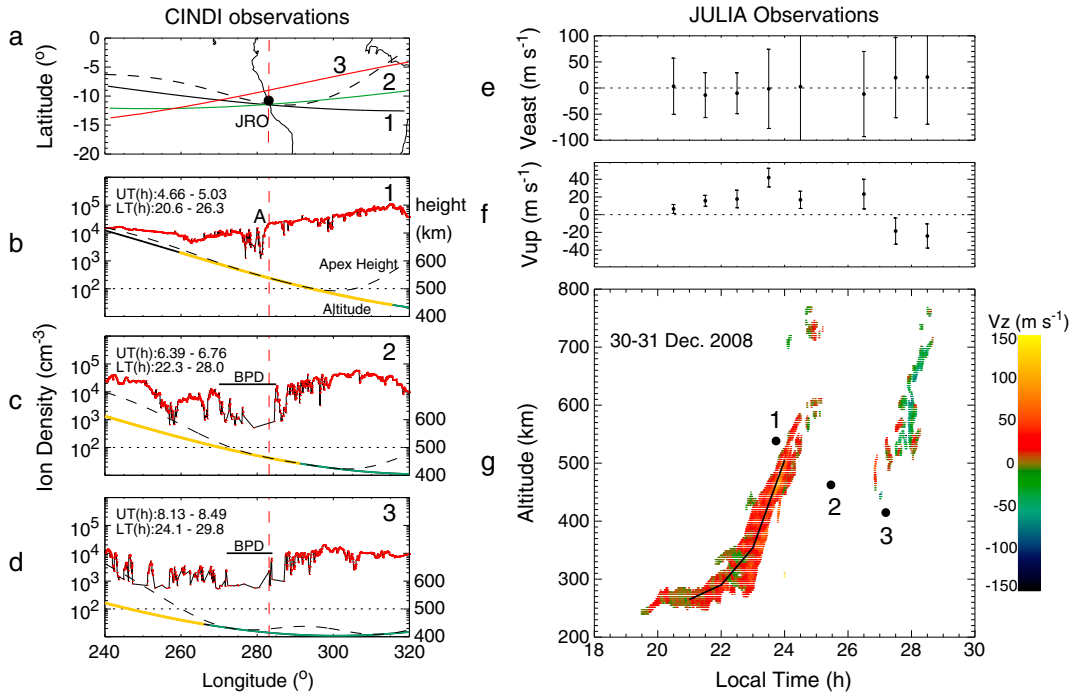

Figure 1. Comparison of the C/NOFS and JULIA observations on 31 December 2008. (a) C/NOFS orbits. (b–d) Ion densities and altitudes along the three C/NOFS orbits. The black, yellow, and green colors on the altitude curves (thick solid curves) indicate the LT intervals of 1800–2200, 2200–0200, and 0200–0600, respectively. The magnetic apex heights are shown with black dashed lines. (e) Altitude-average eastward velocity of the backscatter echoes. (f) Altitude-average upward velocity of the backscatter echoes. The vertical bars are the standard deviations of the velocity. (g) Vertical velocity map of the backscatter echoes. The C/NOFS orbits over JRO are indicated with black solid dots. The black curve inside the backscatter echoes before midnight shows the height estimated from the vertical velocity of the backscatter echoes.

(positive is upward) velocities of the irregularities derived from the radar observations are shown in Figures 1e and 1f, respectively. The vertical bars are the standard deviations of the velocity. In Figure 1g, the C/NOFS altitudes over JRO are indicated with black solid dots. In Figures 1c and 1d, the locations of BPDs are indicated using black horizontal bars. Deep depletions broader than a few degrees in longitude may also be categorized as BPDs. This study focuses on large BPDs. On C/NOFS orbits 2 and 3, the measurements of the ion density over broad longitude regions near JRO are unavailable because the density is below the detection limit. The low density below the detection limit is considered to be caused by the uplift of the bottomside above the C/NOFS altitude. If the uplift is associated with bubbles, large plumes are expected to be detected by JULIA.

[6] On orbit 1, plasma depletions (or bubbles) are not detected at the location of JRO, although deep depletions appear west of JRO. One of the well-known characteristics of bubbles is the elongation along the magnetic field lines. Because of the elongated nature of bubbles, the same bubbles are traceable on consecutive passes of low-inclination orbit satellites [*Huang et al*., 2011; *Kil et al*., 2004]. In a comparison of the C/NOFS observations in Figures 1b–1d, the irregularities detected on one orbit do not match those detected on the other orbits, although the satellite orbits are close to each other and very large plasma depletions appear along those orbits. The different density structures on consecutive orbits may be attributed to the temporal and spatial evolution of the irregularities or to the difference of orbits. However, the inconsistency of the irregularities on consecutive orbits may also be understood as the characteristics of the irregularities in the bottomside. The irregular density fluctuations are similar to those observed below an altitude of 300 km by the Atmosphere Explorer-E satellite [*Kil and Heelis*, 1998].

[7] On the vertical velocity map in Figure 1g, upward movements of backscatter echoes are observed before 2500 LT. The altitude of C/NOFS orbit 1 is slightly above those upward-moving backscatter echoes. This observation is consistent with the absence of bubbles over JRO in Figure 1b. The upward-moving backscatter echoes between 2230 and 2500 LT in the altitude range of 300–600 km can be interpreted as either a slanted plume or an irregularity layer in the bottomside. Our interpretation is the latter. If the backscatter echoes are produced by a plume associated with a bubble, the candidate bubble is the deep plasma depletion detected west of JRO (indicated with a character "A" in Figure 1b). For the appearance of this depletion over JRO about 20 min after the C/NOFS pass (orbit 1), the depletion should drift eastward with a velocity greater than 150 m s^{-1}. However, the zonal velocity of the irregularities at premidnight is near zero, as we can see in Figure 1e. The observations of plasma motion in the Peruvian sector show that the zonal drift velocities of meter-scale irregularities, large-scale (several tens of kilometers) irregularities, and background ionosphere are similar [e.g., *Fejer et al*., 1985; *Martinis et al*., 2003]. Therefore, the zonal velocity of meter-scale irregularities observed by JULIA represents the zonal motion of the irregularities and background ionosphere. Considering the zonal plasma drift, bubbles that match the backscatter echoes before midnight do not appear in the CINDI observations. Thus, the

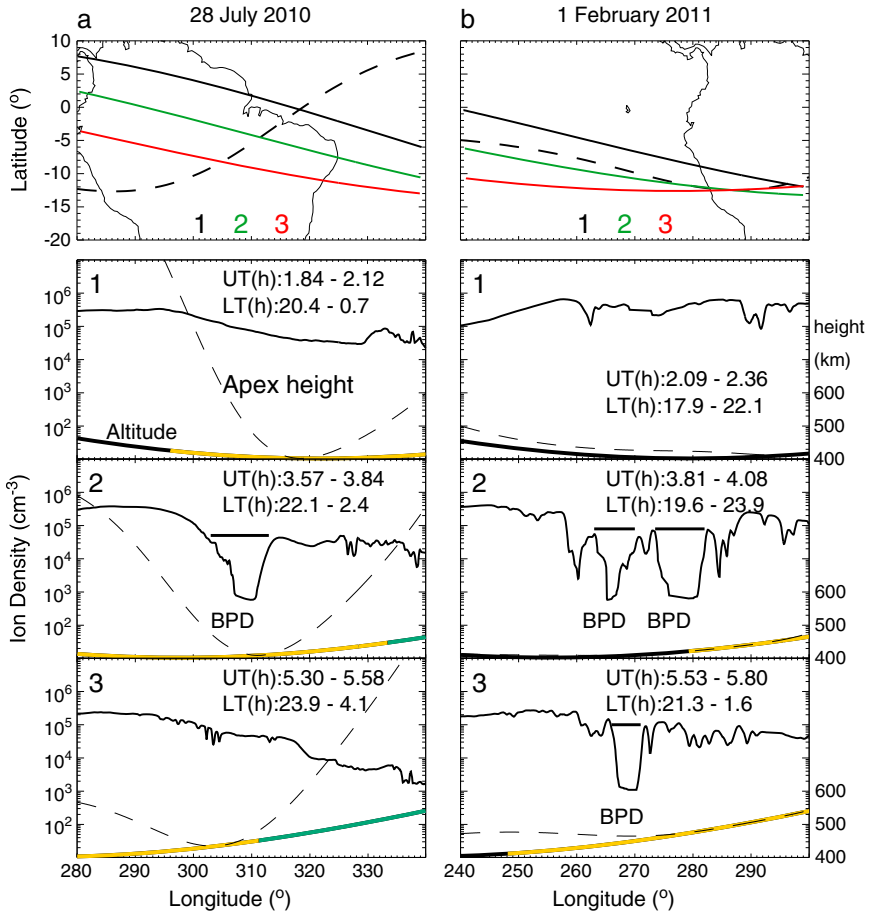

Figure 2. C/NOFS observations of the ion density on (a) 28 July 2010 and (b) 1 February 2011. The color curves in the density plots show the C/NOFS altitude. LT intervals of 1800–2200, 2200–0200, and 0200–0600 are shown with black, yellow, and green colors, respectively, on the altitude curves (thick solid curves). The magnetic apex heights are shown with black dashed lines.

backscatter echoes before midnight are considered to be associated with the bottomside irregularity layer.

[8] Assuming the backscatter echo to be a tracer of the vertical movement of the ionosphere, we can estimate the change of the *F* region height. The black curve inside the backscatter echoes at premidnight shows the height change calculated from the average velocity shown in Figure 1f. The calculated height is consistent with the height of the backscatter echoes. If our interpretation of the backscatter echo is correct, C/NOFS orbit 1 is above the bottomside irregularity layer, and orbits 2 and 3 are below the bottomside irregularity layer. The backscatter echoes detected above an altitude of 700 km around 2500 LT and above C/NOFS orbit 3 around 2800 LT look like plumes (or bubble signatures). The ionospheric uplift provides a preferred condition for the generation of bubbles, and therefore, the coincidence of bubbles and BPDs is expected. The ionosonde observations at JRO showed the existence of spread *F* before midnight and the increase of the occurrence height of spread *F* until midnight. These observations are consistent with the observations of JULIA. No return signal was observed after midnight by the ionosonde. Considering the absence of a plume structure in the JULIA observation, bubbles are excluded from the source of the low plasma density after midnight. Then the fountain process is the plausible mechanism of the equatorial plasma depletion. The JULIA observation of the upward motion of the irregularities and the ionosonde observation of the increase of the spread *F* height are interpreted as evidence of uplifting of the irregularity-embedded ionosphere. Unfortunately, the incoherent scatter radar observation at JRO was not available on 31 December 2008.

[9] To further investigate the BPD characteristics and the association of BPDs with bubbles, we present two examples of BPDs detected by CINDI. Figure 2a presents the observations on 28 July 2010. On the map, three C/NOFS orbits are shown with solid lines, and the location of the magnetic equator is marked with a dashed line. The ion densities along the C/NOFS orbits are presented in the bottom three panels. The color curves in the density plots show the C/NOFS altitude on a linear scale. LTs in the intervals of 1800–2200, 2200–0200, and 0200–0600 are shown with black, yellow, and green colors, respectively, on the altitude curves. The magnetic apex heights are shown using black dashed lines. A BPD is detected near midnight when C/NOFS (orbit 2) passes near the magnetic equator. The longitudinal width of the BPD at the middle of the depletion is about 7°. No bubble signature is found on the earlier (orbit 1) and later (orbit 3) orbits at the longitude of the BPD detection. This BPD event is seen to be a local phenomenon confined to low altitudes and near the magnetic equator. Although the magnetic latitudes of orbits 2 and 3 are similar at the longitude (~308°E) of the BPD detection, no irregularity is detected on orbit 3.

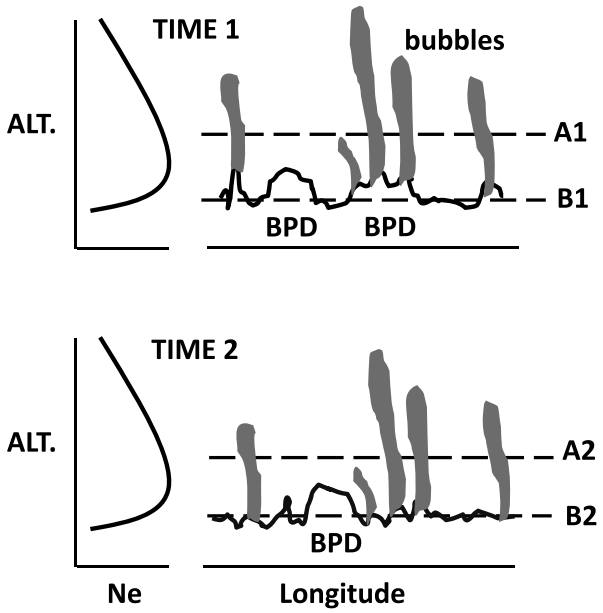

Figure 3. Schematic illustration of the detection of BPDs and irregularities depending on the satellite height.

If the BPD were associated with bubbles, the bubbles that were responsible for such a large depletion would be persistent for one orbital period (90 min) and would be detected on orbit 3. The altitude of orbit 3 is only 30 km higher than that of orbit 2 at the longitude of 308°E. We cannot rule out the possibility of the creation of bubbles, formation of a BPD by a merger of bubbles, and decay of the BPD between orbits 1 and 3. However, an alternative interpretation is that the BPD is not associated with bubbles. If the *F* peak height in the equatorial region was lifted at midnight above an altitude of 450 km, the sampling of the bottomside by CINDI would produce the BPD. The observation of an unstructured BPD (absence of small-scale irregularities) supports the idea that the BPD is not associated with bubbles. The detection of an unstructured BPD is interpreted as an indication of the absence of the irregularities in the bottomside.

[10] Figure 2b is the same format as Figure 2a for the observations on 1 February 2011. Orbit 1 is parallel to the magnetic equator at about 4° magnetic north. The time and altitude of orbit 1 near 270°E longitude are 2000 LT and 400 km. Plasma depletions are detected near the longitudes of 262° and 290°E on orbit 1. However, no depletion is detected at the longitude of 278°E, where a BPD is detected on orbit 2. Along orbit 2, which is very close to the magnetic equator, BPDs are detected. The detection altitudes of BPDs are close to 400 km. The location of one BPD is close to JRO, but, unfortunately, JULIA observation was not available on that day. On orbit 3, one BPD is detected near 268°E at an altitude of 430 km. The occurrence longitude of the BPD on orbit 3 does not coincide with the longitudes of BPDs detected on orbit 2. The signature of the BPD detected at the longitude of 278°E on orbit 2 does not appear on orbit 3. At 278°E, the latitude difference between orbits 2 and 3 is less than 2°, but the altitude difference between the two orbits is 50 km. The detection of BPDs along the orbit close to the magnetic equator and at low altitudes is similar to the observations on 28 July 2010. The irregularities detected along the three consecutive orbits look uncorrelated, although the orbits are close to the magnetic equator. The BPD events presented in Figure 2 indicate that BPDs are confined to regions near the magnetic equator at low altitudes and are not persistent for one orbital period. These BPD characteristics and the results presented in Figure 1 are better explained by assuming that BPDs are not associated with bubbles than by assuming that bubbles are responsible for BPDs.

[11] Our understanding of the BPD phenomenon and irregularities is schematically illustrated in Figure 3. The diagram is similar to one in *Su et al*. [2002] that illustrates BPDs during a large geomagnetic storm. In Figure 3, the altitudinal ion density profile is shown on the left, and the longitudinal density structures are shown on the right. Satellite orbits on the topside and bottomside are denoted with horizontal dashed lines. The rugged thin lines represent the bottomside irregularity layer, and vertical structures represent bubbles. At TIME 1, topside orbit A1 detects only grown bubbles. After one orbit period (TIME 2), the satellite may detect similar irregular structures or bubbles if its orbit (A2) is maintained on the topside. Because of the elongation of bubbles along the magnetic field lines, the topside orbit may detect similar structures off the magnetic equator. When the satellite is below the *F* peak height (orbit B1), the satellite detects two BPDs and rugged irregularities. At TIME 2, the bottomside irregularity layer is changed, although the plume structures in the topside are persistent. As a result, the BPD and small-scale irregularities detected along B2 do not match those detected along B1. Because the uplift of the bottomside provides a preferential condition for the creation of bubbles, the coincident observations of bubbles and BPDs are normal. However, the uplift of the bottomside does not guarantee the creation of bubbles, and BPDs may not always accompany bubbles. The observations on 28 July 2010 (Figure 2a) demonstrate this case.

3. Conclusions

[12] We report BPD events that are not associated with bubbles. The comparison of the coincident C/NOFS and radar observations over JRO on 31 December 2008 shows the occurrence of BPDs at the time when backscatter echoes are absent and at the height below backscatter echoes. The development of BPDs in the absence of bubbles is also identified from the C/NOFS observations on 28 July 2010 and 1 February 2011. These observations lead us to the conclusion that bubbles were not a prerequisite for those BPDs. We understand those BPDs in terms of the uplift of the *F* peak height above the C/NOFS orbit. The detection of BPDs close to the magnetic equator and at low altitudes and the observation of the uplift of the bottom-type irregularity layer support this idea. BPDs and small-scale irregularities accompanying BPDs do not seem to maintain their identity during one orbital period of the satellite. This property may reveal the spatially localized and temporally variable nature of the bottomside irregularity layer. We note that the reported BPD events do not represent the general properties of BPDs. The characteristics of the bottomside irregularity layer require further investigation. Our upcoming study will be extended for those investigations.

[13] **Acknowledgments.** H. Kil acknowledges support from National Science Foundation Aeronomy program (AGS-1237276). CINDI data are provided through the auspices of the CINDI team at the University of Texas at Dallas supported by NASA grant NAS5-01068. The Jicamarca Radio Observatory is a facility of the Instituto Geofísico del Perú operated with support from National Science Foundation Cooperative Agreement AGS-0905448 through Cornell University.

References

Basu, S., S. Basu, F. J. Rich, K. M. Groves, E. MacKenzie, C. Coker, Y. Sahai, P. R. Fagundes, and F. Becker-Guedes (2007), Response of the equatorial ionosphere at dusk to penetration electric fields during intense magnetic storms, *J. Geophys. Res.*, *112*, A08308, doi:10.1029/2006JA012192.

Burke, W. J., O. de La Beaujardière, L. C. Gentile, D. E. Hunton, R. F. Pfaff, P. A. Roddy, Y.-J. Su, and G. R. Wilson (2009), C/NOFS observations of plasma density and electric field irregularities at post-midnight local times, *Geophys. Res. Lett.*, *36*, L00C09, doi:10.1029/2009GL038879.

de La Beaujardière, O., et al. (2009), C/NOFS observations of deep plasma depletions at dawn, *Geophys. Res. Lett.*, *36*, L00C06, doi:10.1029/2009GL038884.

Fejer, B. G., E. Kudeki, and D. T. Farley (1985), Equatorial *F* region zonal plasma drifts, *J. Geophys. Res.*, *90*(A12), 12,249–12,255.

Greenspan, M. E., C. E. Rasmussen, W. J. Burke, and M. A. Abdu (1991), Equatorial density depletions observed at 840 km during the great magnetic storm of March 1981, *J. Geophys. Res.*, *96*, A8, doi:10.1029/91JA01264.

Huang, C.-S., O. de La Beaujardière, P. A. Roddy, D. E. Hunton, R. F. Pfaff, C. E. Valladares, and J. O. Ballenthin (2011), Evolution of equatorial ionospheric plasma bubbles and formation of broad plasma depletions measured by the C/NOFS satellite during deep solar minimum, *J. Geophys. Res.*, *116*, A03309, doi:10.1029/2010JA015982.

Huang, C.-S., J. M. Retterer, O. de La Beaujardière, P. A. Roddy, D. E. Hunton, J. O. Ballenthin, and R. F. Pfaff (2012), Observations and simulations of formation of broad plasma depletions through merging process, *J. Geophys. Res.*, *117*, A02314, doi:10.1029/2011JA017084.

Hysell, D. L., and J. D. Burcham (1998), JULIA radar studies of equatorial spread *F*, *J. Geophys. Res.*, *103*, A12, doi:10.1029/98JA02655.

Kil, H., and R. A. Heelis (1998), Global distribution of density irregularities in the equatorial ionosphere, *J. Geophys. Res.*, *103*, doi:10.1029/97JA02698.

Kil, H., and L. J. Paxton (2006), Ionospheric disturbances during the magnetic storm of July 15, 2000: Role of the fountain effect and plasma bubbles for the formation of large equatorial plasma density depletions, *J. Geophys. Res.*, *111*, A12311, doi:10.1029/2006JA011742.

Kil, H., S.-Y. Su, L. J. Paxton, B. C. Wolven, Y. Zhang, D. Morrison, and H. C. Yeh (2004), Coincident equatorial bubble detection by TIMED/GUVI and ROCSAT-1, *Geophys. Res. Lett.*, *31*, L03809, doi:10.1029/2003GL018696.

Kil, H., L. J. Paxton, Y. Zhang, S.-Y. Su, and H. C. Yeh (2006), Characteristics of the storm-induced big bubbles (SIBBs), *J. Geophys. Res.*, *111*, A10308, doi:10.1029/2006JA011743.

Martinis, C., J. V. Eccles, J. Baumgardner, J. Manzano, and M. Mendillo (2003), Latitude dependence of zonal plasma drifts obtained from dual-site airglow observations, *J. Geophys. Res.*, *108*(A3), 1129, doi:10.1029/2002JA009462.

Su, S.-Y., H. C. Yeh, C. K. Chao, and R. A. Heelis (2002), Observation of a large density dropout across the magnetic field at 600 km altitude during the 6–7 April 2000 magnetic storm, *J. Geophys. Res.*, *107*(A11), 1404, doi:10.1029/2001JA007552.